Indian Journal of Fibre & Textile Research
Vol. 43, June 2018, pp. 203-208

Study of cyclic bursting loading on needle-punched nonwovens: Part II – Change in air permeability and compression behavior

Bipin Kumar[a], Apurba Das, Atul Sharma, Jagatheesan Krishnasamy & R Alagirusamy

Department of Textile Technology, Indian Institute of Technology Delhi, New Delhi 110 016, India

Received 8 February 2016; revised received and accepted 3 June 2016

Efforts have been made to investigate the physical properties of needle-punched nonwovens, such as compression and air permeability, before and after the application of cyclic bursting pressure. It is observed that the structural parameters, such as areal density, needling density and fibre fineness, have significant effect on the aforementioned fabric characteristics. More compression is observed in a sample with low mass density. Sample made of coarser fibre shows lower compression as compared to finer fibre samples. The air permeability decreases with increase in mass density. On conducting cyclic bursting test on a sample, the values of air permeability and compression change significantly. The cyclic parameters, such as pressure magnitude and rest time at cyclic peak pressure, cause significant structural changes and reorientation of the fibre during deformation. Increase in pressure and rest time causes increase in compression parameter (α) and air permeability. Nevertheless, at low cyclic pressure level (10% of bursting pressure), the network becomes compact due to fibrous reorientation, and therefore both the values of compression parameter (α) and air permeability show initial drop. On examining the samples made of coarser and finer fibres, the variation is observed in the extent of change in the air permeability.

Keywords: Air permeability, Bursting strength, Compression behaviour, Cyclic pressure, Needle-punched nonwovens

1 Introduction

Nonwoven fabrics are subjected to repeated loading and unloading when used in geotextiles, filters, apparel and for other industrial applications[1]. The effect of cyclic loading brings about change in compression, transmission and air permeability of the fabrics. It is because when fabrics are acted upon by multidirectional force it brings about change in fibre to fibre contact distance, causes fibre slippage & breakages, and possibly changes the pore size distribution[2]. It is therefore expected that the multidirectional loading could bring significant change in the properties of fabrics. Therefore, it becomes essential to study the aforementioned characteristics of the nonwovens under cyclic loading. Several researchers have examined the air permeability and compressional characteristics of the nonwoven fabrics. Zhu *et al*.[3] observed that the air permeability of nonwoven fabrics decreases with the increase in thickness and density of samples. Cincik *et al*.[4] studied the effect of needling density, and blend proportion on the air permeability of the polyester/viscose blended needle-punched nonwovens fabric. The results showed that the air permeability of the fabrics decreases with the increase in mass per unit area. Also they found synergistic effect of the needling density on the air permeability. In another study conducted by Rawal[5], it has been found that the pore size decreases with an increase in fibre volume fraction and the number of layers. Das *et al*.[2,6] described about the effect of cyclic bursting pressure on air permeability of spunbonded nonwoven fabric and found that the air permeability increases after application of cyclic bursting pressure. The application of cyclic outward pressure results in distortion of fabric structure and opening of structural consolidation, and finally causes the breakage of inter-fibre bonds, consequently increasing the air permeability of fabric and compression property.

In addition to air permeability, compression behaviour of nonwoven fabric plays an important role in the various applications such as geotextiles, carpet, etc. Compression may be defined as the decrease in thickness of fabric with the application of pressure. The compression characteristics depend on the fibre slippage, bending and degree of fibre entanglement. During the application of compressive load, the inter-fibre frictional forces are overcome beyond a limit which results in slippage of fibre. The compression parameter (α) is frequently used in literature to explain the compression and recovery property of nonwovens[7,8]. Higher value of (α) indicates more percentage change in thickness

[a]Corresponding author.
E-mail: bipiniitd18@gmail.com

during compression loading of a sample[7]. Understanding of the change in compression parameter α after bursting could be useful in evaluating the nonwoven performance.

In the earlier part[9], we have discussed about the distension behaviour of the fabrics at different proportion of bursting pressure and rest time at peak pressure on different samples. The proportions of bursting pressures selected were 10 %, 20% and 30% of actual bursting strength of individual fabric. In this study, the air permeability and compression characteristics of different needle-punched nonwovens are examined under cyclic bursting loading.

2 Materials and Methods

2.1 Materials

The materials used for this study are given in Table 1. Polypropylene fibre having two different deniers (15 and 6) was used. The mass per unit area of 200, 300 and 400 g/m^2, and the needling density of 60, 140 and 220 punches/cm^2 were used.

2.2 Measurement of Air Permeability and Compression

ASTM D-737 standard was used for measuring air permeability. The readings were obtained by TEXTEST FX 3300 Air Permeability Tester at 125 Pa (cm^3/cm^2/ s). Air was drawn through the fabrics by means of suction pump. The test area was 5.07 cm^2. The results of air permeability before cyclic test are shown in Table 2.

The fabric thickness and compression test were performed on an Essidel thickness tester. The fabrics were placed on an anvil and pressure foot of 20 mm diameter was brought down to apply a pressure. The compressive load was increased in steps (from 2 kPa to 20 kPa), and the corresponding thicknesses were recorded after waiting for 30s at each pressure level. The

Table 1 — Details of needle-punched nonwoven polypropylene fabrics [Depth of needle penetration = 10mm]

Sample No.	Fibre linear density, den	Mass per unit area, g/m^2	Punch density punches/cm^2
S1	15	200	60
S2	15	200	140
S3	15	200	220
S4	15	300	60
S5	15	300	140
S6	15	300	220
S7	15	400	60
S8	15	400	140
S9	15	400	220
S10	6	200	60
S11	6	200	140
S12	6	200	220
S13	6	300	60
S14	6	300	140
S15	6	300	220
S16	6	400	60
S17	6	400	140
S18	6	400	220

Table 2 — Experimental test results

Fabric	Measured mass per unit area, g/m^2		Thickness, mm		Bursting strength, kg/cm^2		Air permeability, cm^3/cm^2/s	
	Avg	CV %	Avg	CV %	Avg	CV %	Avg	CV %
S1	221.10	3.08	3.64	3.76	17.12	2.34	335.15	8.14
S2	225.30	6.28	3.69	8.4	12.80	6.08	317.32	14.25
S3	220.97	5.63	3.38	3.56	10.42	4.53	293.40	10.51
S4	306.25	5.98	5.26	4.17	23.16	2.70	238.41	12.55
S5	304.30	3.26	5.17	3.42	20.16	3.57	217.55	9.81
S6	292.12	4.49	4.47	3.38	19.18	4.58	229.61	8.59
S7	403.27	4.84	6.12	6.44	29.31	4.73	182.20	7.28
S8	389.05	3.69	5.61	4.30	27.56	3.21	163.76	9.43
S9	393.40	2.76	5.05	3.02	22.48	6.66	179.40	8.31
S10	184.41	3.61	3.10	3.10	19.32	4.29	202.16	5.78
S11	187.90	1.89	2.79	2.79	13.66	3.05	150.66	9.51
S12	184.13	6.79	2.53	2.53	11.61	4.74	176.50	7.59
S13	304.25	8.09	4.37	4.37	26.70	6.83	112.83	2.88
S14	316.10	6.25	4.28	4.28	25.48	6.31	106.66	1.41
S15	309.10	2.06	3.71	3.71	24.23	6.25	111.00	5.19
S16	414.63	4.91	4.88	4.88	35.31	6.66	109.40	5.06
S17	403.06	4.30	4.93	4.93	30.98	7.61	92.40	5.29
S18	395.64	1.70	4.73	4.73	28.86	2.04	98.13	4.89

Avg – Average; CV – Coefficient of variation.

initial and final thickness at lowest pressure [2 kPa (P_i)], and highest pressure [20 kPa (P_f)] are termed as T_0 and T_f respectively. The thickness of the specimen at a given load during compression and recovery can be expressed as[7,8]:

$$\frac{T}{T_o} = 1 - \alpha \ln\left(\frac{P}{P_o}\right) \quad \ldots (1)$$

$$\frac{T}{T_f} = 1 - \beta \ln\left(\frac{P}{P_f}\right) \quad \ldots (2)$$

where α and β are the compressional and recovery parameters respectively. Using the thickness-pressure plot, one can also obtain work done during compression (E_c) and recovery (E_r) by calculating areas under curves (Fig. 1). Finally, the energy loss (E_L) during the cyclic compression can be obtained as

$$E_L = \frac{E_c - E_r}{E_c} \quad \ldots (3)$$

This parameter (E_L) is a good indicator for assessing the resiliency of nonwovens for different technical applications[7,8]. A lower E_L represents better compression resiliency of the sample. Table 3 shows the values of α and E_L observed for all samples using above equations. For the significance test, ANOVA analysis was also done. The parameters with p-value lower than 0.05 is considered to have significant effect on the fabric properties.

3 Results and Discussion

3.1 Air Permeability

Before Cyclic Bursting Loading

The effect of areal density and punch density was observed on the air permeability of the fabrics. Table 2 shows the decrease in air permeability with increase in areal density of samples. As an example, the air permeability values for samples S1 (100 g/m²), S4 (200 g/m²) and S7 (300 g/m²) are found 335.1, 238.4 and 186.2 cm³/cm²/s respectively. This is because of the increase in available fibrous surface area which enhances the flow resistance for passing air[8].

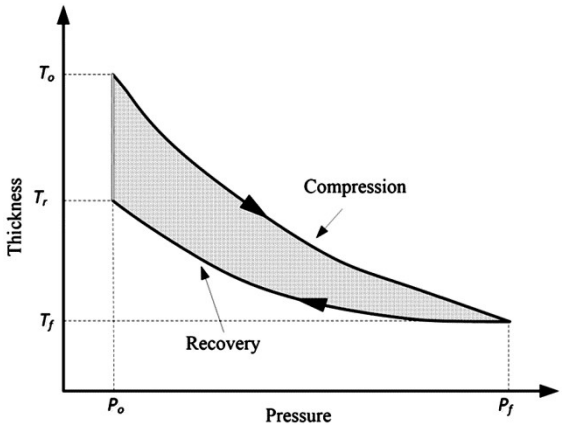

Fig. 1 — Representative curve obtained during compression load-recovery cycle (shaded portion represents the energy loss in the cyclic process)

The trend for air permeability is not found significant for needling density ($p>0.05$) (Table 4). At lower mass density (100 g/m²), the permeability values for samples S1 (60 punches/cm^2), S2 (140 punches/cm^2) and S3 (220 punches/cm^2) are 335.1, 317.3 and 293.4 cm³/cm²/s respectively, following a decreasing trend. However, for higher mass samples (300 and 400 g/m^2), the permeability first decreases and then increases with needle punch density. The needle density affects the fibrous reorientation in the fabric structure, primarily favours more entanglement to develop a compact structure[8,10]. However, more punching could have adverse effect and may cause significant fibre breakages. This could be even worse for heavier samples (300 and 400 g/m^2), where more fibre breakages are bound to happen due to availability of more fibres per unit area during punching. Porometry results (Table 5) also show a lower mean flow pore size at 220 punches/cm^2 compared to 140 punches/cm^2 for higher mass samples (300 and 400 g/m^2). This confirms the reduction in air permeability at 220 punches/cm^2 for heavier samples.

For same areal and needling density, the air permeability is more for coarser fibre (15 denier) as compared to that for finer fibre (6 denier). This can be

Table 3 — Results of compression parameters

Fabric	Compression parameter (α)	Energy loss (E_L), %
S1	0.148	27.38
S2	0.137	25.97
S3	0.122	25.26
S4	0.146	27.35
S5	0.133	25.79
S6	0.120	25.07
S7	0.157	28.87
S8	0.148	27.45
S9	0.143	27.12
S10	0.158	30.14
S11	0.156	29.22
S12	0.146	27.51
S13	0.154	29.45
S14	0.148	28.11
S15	0.141	26.78
S16	0.167	30.87
S17	0.158	30.11
S18	0.155	29.56

Table 4 — ANOVA analysis for the significance of structural parameters on air permeability

Source	Sum of square	Degree of freedom	Mean square	F	Prob>F
Fibre denier**	55229.4	1	55229.4	149.29	0
Mass density**	37198	2	18599	50.27	0.0001
Needle density	1523.9	2	762	2.06	0.1702
Error	4439.5	12	370		
Total	98390.8	17			

**The factors significant at 95% level of confidence.

Table 5 — Mean pore size of samples using porometry (ASTM F 316-03)

Sample	Mean flow pore size, μm	
	Before bursting	After bursting[a]
S1	150.46	176.35
S2	128.36	145.43
S3	115.56	135.64
S4	130.46	150.47
S5	110.34	123.51
S6	113.32	122.11
S7	114.42	126.54
S8	96.24	99.48
S9	98.32	99.87
S10	75.43	82.38
S11	62.53	69.41
S12	55.45	60.87
S13	60.67	72.10
S14	50.13	57.32
S15	50.85	57.91
S16	49.89	53.24
S17	39.89	47.54
S18	40.16	46.67

[a]Pressure level – 30% of bursting pressure.

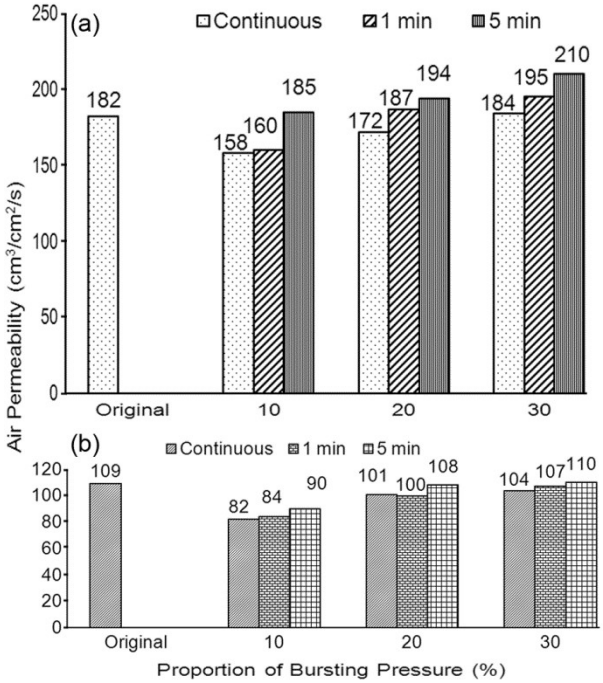

Fig. 2 — Effect of cyclic bursting pressure on air permeability for different fabric samples (a) S7 (15 den) and (b) S16 (6 den)

explained by the fact that the total number of fibres presents in the network decreases for coarser fibre compared to that for finer fibre denier, keeping levels of other factors same (i.e. mass and needle density). This decreases the total exposed surface area, and therefore low resistance to the air passage for coarser fibre[8] ($p<0.05$) (Table 4).

After Cyclic Bursting Loading

After conducting repeated cyclic bursting, air permeability of each sample is also observed and analysed. To summarize the results, herein we are describing the behaviour of two representative samples, one from the group of 15 denier (S7) and other from 6 denier (S16). Increase in pressure magnitude causes increase in the air permeability. Figure 2(a) shows the results where it can be observed that after cyclic test the highest value is measured at 30% bursting pressure and lowest at 10% pressure for same rest time. Cyclic bursting results in significant structural changes in the fibrous network. With increases in pressure magnitude, it is expected to have more severe action on the fibrous network. More pressure causes greater distortion of fabric structure and breakage due to distension of fibre and breakage of inter fibre bonds which may increase pore sizes. To confirm this results, the pore characteristics are obtained using a porometer (Model: POROLUX^{TM} 500; Standard: ASTM F 316-03; Table 5). As an example, the values of the mean flow pore size for Sample S16 after continuous cyclic tests are 45.2, 47.8 and 53.2 μm respectively at 10, 20 and 30% pressure levels. Similar trend is observed for other samples.

Examining the magnitude of air permeability before and after cyclic bursting, it is found that the air permeability observed at 10% pressure level is lower than its original value [Fig. 2(a)]. Similar observation is found for all other samples. Primarily, there are two processes working together during bursting pressure viz

first the structural deformation due to fibre breakages or slippages which might increase mean pore size; and second the fibrous realignment or entanglement for structural consolidation. At low pressure level (10%), the extent of structural deformation is less but the fibre gets realigned and reorient on the fabric surface which provide more resistance to air flow. This is further confirmed form the results of mean pore size which get reduced after conducting bursting test (at 10% pressure level). The mean flow pore size values for Sample S7 before and after cyclic test (at 10% pressure level; continuous cycle) are 57.4 and 45.2 μ_m respectively. Similar results are also observed for 6 denier sample S16 [Fig. 2(b)] at low 10% pressure level. Similar to the effect of pressure magnitude, more distension is observed with increasing rest time as mentioned earlier[9], and therefore air permeability after bursting test is highest for 5 min (Fig. 2) for same pressure magnitude.

On comparing the results of coarser and finer fibres, it has been found that the extent of change in air permeability is more for 6 denier as compared to that for 15 denier at lower pressure level (Fig. 2). For example, at low pressure level (10%) and zero rest time, the percentage reduction of air permeability is 24.7% for 6 denier, whereas it is 13.1% for 15 denier. This indicates more structural consolidation for a sample made of 6 denier. This is attributed due to fact that more fibres are available for entanglement and reorientation on the fabric surface in a finer fibre samples as compared to coarser fibre sample if other structural parameters (mass and needling density) are kept the same. In addition, another observation can also be made if the effect of rest time is considered for coarser and finer samples. In this case, the trend is opposite as compared to the effect of pressure magnitude. As explained above, the rest time increases the air permeability due to permanent deformation in the fabrics, i.e. creep. However, the change is less prominent for 6 denier as compared to 15 denier. As an example, when compared the air permeability values between zero (continuous) and 5 min rest time at 10% pressure level, the percentage increase is 9.7% and 17.1% respectively for 6 denier and 15 denier samples (Fig. 2). This could be explained by the fact that lesser creep deformation is expected in a sample made of finer fibre. More number of fibres are available in a sample made of 6 denier as compared to that in 15 denier sample, and hence results in more entanglement which provide more frictional resistance to fibre slippages during creep.

3.2 Compressional Behaviour

Before Cyclic Bursting Loading

The initial results of compression performance of the needle-punched nonwoven fabric sample are shown in Table 3. The result is expressed in dimensionless parameters (α and E_L) as described in Eq. (1). High value of α indicates more extent of thickness reduction. From the results of selected samples (S2, S5 and S8) with varying mass density, it has been found that the compression parameter α first decreases and then increases. The α values are 0.137, 0.133 and 0.148 respectively for 200 g/m^2 (S2), 300 g/m^2 (S5) and 400 g/m^2 (S8) respectively. Increasing the mass density from 200 g/m^2 to 300 g/m^2, more number of fibres are present in the path of penetrating needle barbs which leads to more entanglement and therefore provides greater frictional resistance for fibre movement. This reduces the compressional behaviour of the fabric. However, if there exists too much fibres for needle punching (as in case of 400 g/m^2), the action of needle barbs might not be sufficient for uniform entanglements throughout in the structure. During production, the depth of needle penetration is kept constant (10 mm), so there is possibility of poor fibre carrying capacity of needle barbs and more fibre breakages could happen in the structure in the case of 400 g/m^2 samples. This could provide non-uniform consolidation for 400 g/m^2 samples, and therefore highest compressibility compared to 200 g/m^2 and 300 g/m^2 samples. Similar trend is also observed for the energy loss E_L.

The increase in punch density decreases the compressibility. Looking to a subset of samples, such as S1 (60 punches/cm^2), S2 (140 punches/cm^2) and S3 (220 punches/cm^2), S1 has highest α (0.148) and S3 has lowest α (0.122). More needle punching leads to more compact fabric structure, and therefore lower compressibility ($p<0.05$) (Table 6). When examining the results of fibre denier, it can be seen that a 15 denier sample has lower α compared to 6 denier, keeping other parameters same ($p<0.05$). Compression test involves significant bending of fibres in the structure, and a 15 denier fibre has larger diameter compared to 6 denier due to which a 15 denier fibre has high bending resistance. This decreases compressibility for sample made of 15 denier fibre.

After Cyclic Bursting Loading

Figures 3 and 4 show the general behaviour of the effect of cyclic bursting on the compression parameter (α) and energy loss (E_T). Similar trends are observed for all other samples. Increase in the pressure magnitude results in increase in α and E_T as shown in Figure 3. High pressure leads to more structural deformation in the structure, leading to weakening of entanglement points, and therefore the sample shows

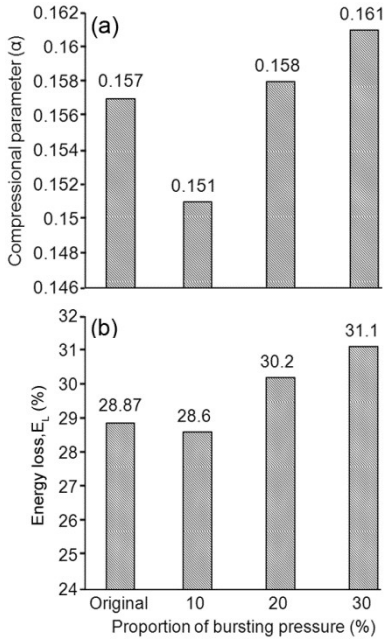

Fig. 3 — Effect of cyclic bursting pressure on (a) compression parameter (α) and (b) energy loss (E_L) for the sample S7

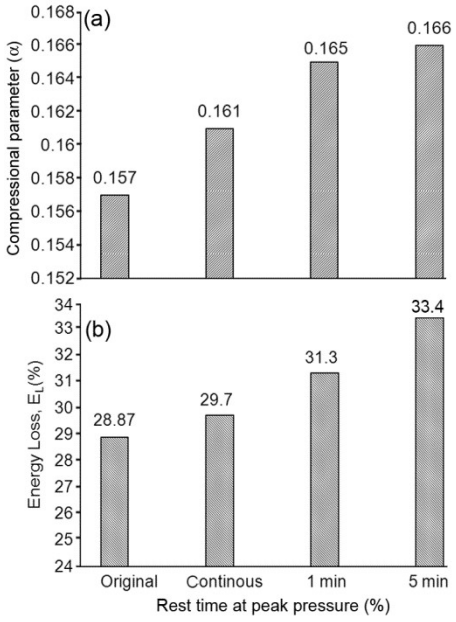

Fig. 4 — Effect of rest time on (a) compression parameter (α), and (b) energy loss (E_L) for the sample S7 at 30% of bursting pressure

increasing compression deformation and more energy loss. Although the α shows increasing trend from 10% to 30% pressure level but at 10% pressure level, the α value (0.151) is lower than the original value (0.157). As discussed above, the structural consolidation is more prominent at low pressure level which may cause a marginal decrease in α and E_T. The effect of rest time at peak pressure has prominent effect on α and E_T. As can be seen from Figure 4, the α and E_T are highest at 5 min. Loading time brings about more structural deformation due to fibre breakage and creep deformation, and this could attribute to the increase in both parameters.

4 Conclusion

The changes in fabric characteristics, such as air permeability and compression, of the needle-punched nonwovens are studied after conducting cyclic bursting loading. Significant change in the fabric characteristics are observed which could be explain from the change in the structural deformation or fibrous reorientation of the fabric that depends on the process parameters and amount of cyclic pressure. An increase in air permeability is observed with increase in proportion of bursting pressure, however at low pressure levels (10%) there is an initial drop in air permeability due to structural consolidation. High rest time at cyclic peak pressure also increases the air permeability. This effect is found to be more prominent in coarser fibre as compared to that in finer fibre. Examining the compression results, it has been found that the compressional parameters (α and E_T), show decreasing trend with increasing needling density, but they show opposite trend with fibre denier. Both the cyclic pressure magnitude and rest time cause increase in α and E_T.

Acknowledgement

The authors would like to acknowledge with thanks the funding support received from the Department of Science and Technology, India.

References

1 Hearle J & Purdy A, *Fibre Sci Technol*, 4(2) (1971) 81.
2 Das A & Raghav R, *Indian J Fibre Text Res*, 36(1) (2011) 53.
3 Zhu G, Kremenakova D, Wang Y & Militky J, *Autex Res*, 15(1) (2015) 8.
4 Çinçik E & Koç E, *Text Res J*, 82(5) (2012) 430.
5 Rawal A, *J Text Inst*, 101(4) (2010) 350.
6 Das A & Raghav R, *Indian J Fibre Text Res*, 35(3) (2010) 258.
7 Kothari V & Das A, *Geotext Geomembr* , 11(3) (1992) 235.
8 Kumar B, Singh J, Das A & Alagirusamy R, *Mater Sci Eng C,* 57 (2015) 215.
9 Kumar B, Das A, Sharma A, Krishnasamy J & Alagirusamy R, *Indian J Fibre Text Res*, 43 (2018) 20.
10 Kumar B, Das A, Pan N, Alagirusamy R, Gupta R & Singh J, *J Biomater Appl* , 30(5) (2015) 589.